

# Search for Standard Model Higgs boson in $H \rightarrow \tau^+\tau^-$ decay with the ATLAS detector

Koji Nakamura<sup>1,a</sup> and on behalf of ATLAS Collaboration

<sup>1</sup>High Energy Accelerator Research Organization (KEK)

**Abstract.** A search for the Standard Model (SM) Higgs boson decaying into a pair of  $\tau$  leptons is presented. The results are based on data samples of proton-proton collisions accumulated by ATLAS experiment at the LHC and corresponding to integrated luminosities of  $4.6 \text{ fb}^{-1}$  and  $13.0 \text{ fb}^{-1}$  at center-of-mass energies of  $\sqrt{s} = 7 \text{ TeV}$  and  $8 \text{ TeV}$ , respectively. The observed (expected) upper limit at 95% C.L. on the cross-section times the branching ratio for SM  $H \rightarrow \tau^+\tau^-$  is found to be 1.9 (1.2) times the SM prediction for a Higgs boson with mass  $m_H = 125 \text{ GeV}$ . For this mass the observed (expected) deviation from the background-only hypothesis corresponds to a local significance of 1.1 (1.7) standard deviations.

## 1 Introduction

The observation of a new particle with a mass of  $125 \text{ GeV}$  by the ATLAS and CMS experiments [1, 2] in the search for the Standard Model (SM) Higgs boson is a great success of the Large Hadron Collider (LHC) physics program and the beginning of a new era in particle physics.

One of most important way to make sure the observed particle is the Higgs boson is to measure its couplings to bosons and fermions and test the prediction of the Standard Model. At the same time as the observation of the new boson, we observed a significant excess with respect to the background in  $H \rightarrow \gamma\gamma$ ,  $H \rightarrow ZZ$  and  $H \rightarrow W^+W^-$ , they strongly indicate the new boson have non-zero coupling to vector bosons. Because the excess of these channels are observed in the search for Higgs boson with gluon fusion productions, they also indicate non-zero coupling of Higgs to quarks.

The SM predicts the Higgs boson coupling to leptons, in particular the  $\tau$  lepton because of its relatively heavy mass. For the Higgs boson with a mass of  $125 \text{ GeV}$ , the  $H \rightarrow \tau^+\tau^-$  channel, with a branching ratio of 6.3% [3], can be observed by data accumulated in LHC experiments. The study of  $H \rightarrow \tau^+\tau^-$  channel across various production processes will ultimately lead to measurements of a number of important Higgs couplings.

The three processes with the largest SM Higgs boson production cross-section at the LHC are gluon fusion  $gg \rightarrow H$  (denoted as ggF),  $W$  or  $Z$  boson fusion  $qq \rightarrow qqH$  (denoted as VBF) and associated production with  $W$  or  $Z$  boson  $qq \rightarrow VH$  (denoted as VH). The cross-section for each processes at 7 and 8 TeV collisions are summarized in Table 1.

This proceeding presents SM Higgs boson searches in the  $H \rightarrow \tau_{\text{lep}}^+\tau_{\text{lep}}^-$ ,  $H \rightarrow \tau_{\text{lep}}^+\tau_{\text{had}}^-$ ,  $H \rightarrow \tau_{\text{had}}^+\tau_{\text{had}}^-$  channels,

<sup>a</sup>e-mail: Koji.Nakamura@cern.ch

**Table 1.** The total production cross section for each production processes at center-of-mass (C.M.) energy 7 and 8 TeV proton-proton collisions [3].

C.M. energy	$gg \rightarrow H$	$qq \rightarrow qqH$	$qq \rightarrow VH$
7TeV	15.3 [pb]	1.22 [pb]	0.89 [pb]
8TeV	19.5 [pb]	1.57 [pb]	1.09 [pb]

where  $\tau_{\text{lep}}^+$  and  $\tau_{\text{had}}^-$  denote leptonically and hadronically decaying  $\tau$  leptons, respectively. The analyses use data samples of proton-proton collisions accumulated by ATLAS experiment at the LHC and corresponding to integrated luminosities of  $4.6 \text{ fb}^{-1}$  and  $13.0 \text{ fb}^{-1}$  at center-of-mass energies of  $\sqrt{s} = 7 \text{ TeV}$  and  $8 \text{ TeV}$ , respectively [4].

## 2 ATLAS experiment and analysis strategy

### 2.1 ATLAS experiment and detector

The ATLAS experiment utilizes a multipurpose detector and it consists of an inner detector surrounded by thin superconducting solenoid, electromagnetic and hadronic calorimeters, and an external muon spectrometer incorporating three large superconducting air-core toroid magnets [5]. Electrons, muons,  $\tau$  leptons, jets and neutrinos (through the presence of missing transverse momentum,  $E_T^{\text{miss}}$ ) can be reconstructed, identified and measured with high precision in the ATLAS detector. The only data taken with all sub-systems relevant to this analysis operational are used.

### 2.2 Event selection

An initial selection of events is performed by requiring a vertex from the primary  $pp$  collisions that is consistent

with the position of the interaction region. Overall quality criteria are applied to suppress events with fake  $E_T^{\text{miss}}$ , produced by non-collision activity such as cosmic ray muons, beam-related backgrounds or noise in calorimeters. Single lepton triggers and combinations of two of lepton or hadronic tau triggers are used to take data, in order to maximize the signal acceptance. Signal events are selected by requiring exactly two opposite-charge tau decay products which are two light leptons (electrons and/or muons, denoted as  $\ell$ ) for  $H \rightarrow \tau_{\text{lep}}^+ \tau_{\text{lep}}^-$  candidate, one light lepton and a  $\tau_{\text{had-vis}}$  (visible component of the hadronically decaying  $\tau$  lepton is denoted as  $\tau_{\text{had-vis}}$ ) for  $H \rightarrow \tau_{\text{lep}}^+ \tau_{\text{had}}^-$  candidate and two  $\tau_{\text{had-vis}}$ 's for  $H \rightarrow \tau_{\text{had}}^+ \tau_{\text{had}}^-$  candidate. The momentum threshold for each tau decay products are determined based on the trigger. To suppress backgrounds produced via purely QCD processes, signal events are commonly selected by requiring large  $E_T^{\text{miss}}$  since tau decay products in signal events include neutrino. The following selections and categorizations are applied for each decay channel differently to reduce backgrounds and to focus on a particular production process. All three channels in this analysis exploit a VBF topology and a Boosted topology which are by requiring large transverse momenta of the  $\ell + \ell + E_T^{\text{miss}}$ ,  $\ell + \tau_{\text{had-vis}} + E_T^{\text{miss}}$ , or a leading jet in the event for  $H \rightarrow \tau_{\text{lep}}^+ \tau_{\text{lep}}^-$ ,  $H \rightarrow \tau_{\text{lep}}^+ \tau_{\text{had}}^-$  or  $H \rightarrow \tau_{\text{had}}^+ \tau_{\text{had}}^-$  channel, respectively. The background processes considered in this search are production of QCD jets,  $W$  and  $Z$  bosons in association with jets ( $W/Z$ -jets), pairs of top quarks ( $t\bar{t}$ ), singly produced top quark, and pairs of electroweak gauge bosons ( $WW, WZ, ZZ$ ). In particular, the  $Z/\gamma^* \rightarrow \tau\tau$  background is the dominant one for this search.

### 2.2.1 $H \rightarrow \tau_{\text{lep}}^+ \tau_{\text{lep}}^-$

To search for a Higgs within the range  $100 \text{ GeV} < m_H < 150 \text{ GeV}$ , the di-lepton invariant mass is required to be in the range  $30 \text{ GeV} < m_{\ell\ell} < 100 \text{ GeV}$  for the  $e\mu$  channel, whereas for the  $ee$  and  $\mu^+\mu^-$  channels  $30 \text{ GeV} < m_{\ell\ell} < 75 \text{ GeV}$  is required to reduce the contamination from  $Z/\gamma^* \rightarrow \ell\ell$ . Events are rejected if there is any jet with  $p_T > 25 \text{ GeV}$  and  $|\eta| < 2.5$  identified as a bottom quark jet. Events are also required to have  $H_T^{\text{miss}} > 40 \text{ GeV}$ , which is missing transverse momentum defined by high- $p_T$  objects<sup>1</sup>,  $0.1 < x_1, x_2 < 1.0$  and the di-lepton azimuthal opening angle  $0.5 < \Delta\phi_{\ell\ell} < 2.5$ , where  $x_1$  and  $x_2$  denote the visible momentum fraction of the  $\tau$  leptons carried by the leading and sub-leading light leptons<sup>2</sup>, respectively.

Five mutually exclusive categories that are characterized by their jet multiplicity and kinematics are defined for this channel : 2-jet VBF, Boosted, 2-jet VH, 1-jet and 0-jet.

1. **2-jet VBF** :  $\Delta\eta_{jj} = |\eta_{j1} - \eta_{j2}| > 3$ ,  $m_{jj} > 400 \text{ GeV}$  and a veto on a third jet with  $p_T > 25 \text{ GeV}$  are required.

<sup>1</sup>identified as electrons muons and jets

<sup>2</sup>For the event selection the momentum of the  $\tau$  lepton is estimated using the collinear approximation [6]

2. **Boosted** :  $p_{T,\tau\tau} > 100 \text{ GeV}$ , where  $p_{T,\tau\tau}$  is the scalar transverse momenta of the di-lepton and  $E_T^{\text{miss}}$  system.
3. **2-jet VH** : Contain two jets with di-jet mass are  $30 \text{ GeV} < m_{jj} < 160 \text{ GeV}$ .
4. **1-jet** : The invariant mass of the two  $\tau$  leptons and the leading jet is required to fulfill  $m_{\tau\tau j} > 225 \text{ GeV}$ .
5. **0-jet** : Only the  $e\mu$  final state. The di-lepton azimuthal opening angle be  $\Delta\phi_{\ell\ell} > 2.5$ .

### 2.2.2 $H \rightarrow \tau_{\text{lep}}^+ \tau_{\text{had}}^-$

To suppress  $W$ -jets and non-resonant background, the transverse mass,  $m_T$ , of lepton and  $E_T^{\text{miss}}$  system, the  $\Sigma\Delta\phi$  variable, defined as  $\Delta\phi_{\ell, E_T^{\text{miss}}} + \Delta\phi_{\tau, E_T^{\text{miss}}}$  and the  $\Delta(\Delta R)$  variable, defined as the difference between the angular separation  $\Delta R_{\ell\tau_{\text{had-vis}}}$ <sup>3</sup> and its expectation value for the Higgs decay, are used. Six exclusive categories are defined for this channel : VBF, Boosted, 1-jet ( $e\tau_{\text{had-vis}}, \mu\tau_{\text{had-vis}}$ ) and 0-jet ( $e\tau_{\text{had-vis}}, \mu\tau_{\text{had-vis}}$ ).

1. **2-jet VBF** :  $\Delta\eta_{jj} = |\eta_{j1} - \eta_{j2}| > 3.0$ ,  $m_{jj} > 500 \text{ GeV}$  and  $p_T^{\text{Total}} < 30 \text{ GeV}$ .
2. **Boosted** :  $p_{T,\tau\tau} > 100 \text{ GeV}$ , where  $p_{T,\tau\tau}$  is the scalar transverse momenta of the lepton,  $\tau_{\text{had-vis}}$  and  $E_T^{\text{miss}}$ . It is also required  $0 < x_1 < 1$  and  $0.2 < x_2 < 1.2$ .
3. **1-jet** : At least one jet with  $p_T > 30 \text{ GeV}$ . The  $e\tau_{\text{had-vis}}$  and  $\mu\tau_{\text{had-vis}}$  final states are considered separately.
4. **0-jet** : No jet with  $p_T > 30 \text{ GeV}$ . The  $e\tau_{\text{had-vis}}$  and  $\mu\tau_{\text{had-vis}}$  final states are considered separately.

### 2.2.3 $H \rightarrow \tau_{\text{had}}^+ \tau_{\text{had}}^-$

Two  $\tau_{\text{had-vis}}$  candidates are required. They must be separated  $0.8 < \Delta R < 2.8$  and  $\Delta\eta < 1.5$ . Two exclusive categories are defined for this channel : VBF, Boosted.

1. **2-jet VBF** :  $\Delta\eta_{jj} = |\eta_{j1} - \eta_{j2}| > 2.6$ ,  $m_{jj} > 350 \text{ GeV}$ .
2. **Boosted** : At least one jet with  $p_T > 70 \text{ GeV}$  and  $\Delta R_{\tau_1\tau_2} < 1.9$ .

## 2.3 Mass reconstruction

The invariant mass is the final discriminating observable used for all channels and is reconstructed by means of the Missing Mass Calculator (MMC) [7]. This technique provides a reconstruction of event kinematics in the  $\tau\tau$  final state with  $> 99\%$  efficiency and  $13 - 20\%$  resolution in  $m_{\tau\tau}$ , depending on the event topology and final state (better resolution is obtained for events with high- $p_T$  jets and boosted topology).

$$^3\Delta R = \sqrt{(\Delta\eta)^2 + (\Delta\phi)^2}$$

$$^4p_T^{\text{Total}} = |\vec{p}_T^\ell + \vec{p}_T^{\tau_{\text{had-vis}}} + \vec{p}_T^{j1} + \vec{p}_T^{j2} + \vec{E}_T^{\text{miss}}|$$

## 2.4 Estimation and modeling of backgrounds

The background composition and normalization are determined using both data-driven and simulation based methods. The main background to the Higgs boson signal in all selected final states is due to the largely irreducible  $Z/\gamma^* \rightarrow \tau\tau$  process. While it is not possible to select a signal-free  $Z/\gamma^* \rightarrow \tau\tau$  sample directly from the data, this background can be modeled in a partly data-driven way by selecting a control sample of  $Z/\gamma^* \rightarrow \mu\mu$  data, where the expected signal contamination is negligible. In this sample the muon tracks and associated calorimeter cells are replaced by simulated  $\tau$  leptons (embedding method). Thus, only the  $\tau$  decays and the corresponding detector response are taken from the simulation, whereas jets, underlying event and all other event properties – including pileup effects – are obtained from data. This procedure has been extensively validated: as an example in figure 1 the obtained MMC mass distribution is compared with simulation.

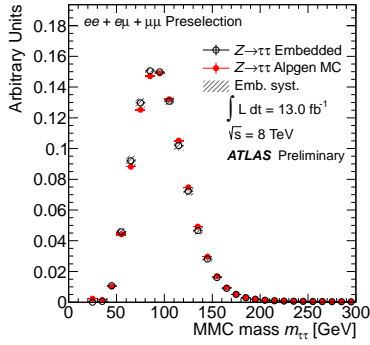


**Figure 1.** Comparison of the MMC mass distribution between embedding and simulation in  $Z/\gamma^* \rightarrow \tau\tau$  background process [4].

The contribution of  $W$ +jets and QCD backgrounds are estimated by data driven method either using template fitting of kinematics distribution or derived from a control regions defined by inverting the opposite charge requirement. The  $t\bar{t}$  and single top backgrounds significantly contribute to the  $H \rightarrow \tau_{\text{lep}}^+ \tau_{\text{lep}}^-$  and  $H \rightarrow \tau_{\text{lep}}^+ \tau_{\text{had}}^-$  channels, thus normalizations are obtained from control regions, defined by inverting the  $m_T$  cut and requiring at least one jet identified as bottom quark jet whereas kinematic shapes are obtained by simulation. The other background estimations are largely relying on the simulation and normalized by data if a control region where the background is enhanced can be defined.

## 2.5 Systematics and signal extraction

Systematic uncertainties which affect the normalization and shape of the signal and background mass distributions are taken into account. These are treated either as full correlated or uncorrelated across categories as appropriate. In the case of partial correlations, the total uncertainty is separated into correlated and uncorrelated components. The dominant correlated systematic uncertain-

ties are those on the measurement of the integrated luminosity and on the theoretical prediction of the signal production cross-sections and decay branching ratios, as well as those related to the detector response to electrons, muons, hadronic  $\tau$ -lepton decays, jets,  $E_T^{\text{miss}}$  and bottom quark identification. Uncorrelated uncertainty across three channels are dominated by background modeling uncertainties. The systematic uncertainties for the  $Z/\gamma^* \rightarrow \tau\tau$  and signal are summarized in table 2 for the three channels separately.

**Table 2.** Summary of  $Z/\gamma^* \rightarrow \tau\tau$  background and signal main systematic uncertainties by channel as main systematic uncertainties. The quoted ranges refer specifically to the 8 TeV dataset, but they are similar for the 7 TeV dataset. Uncertainties indicated with (S) are also applied bin-by-bin, and therefore affect the shape of the final distributions. Signal systematic uncertainties are derived from the sum of all signal production modes.

Uncertainty	$\tau_{\text{lep}}^+ \tau_{\text{lep}}^-$	$\tau_{\text{lep}}^+ \tau_{\text{had}}^-$	$\tau_{\text{had}}^+ \tau_{\text{had}}^-$
$Z/\gamma^* \rightarrow \tau\tau$			
Embedding	1–4% (S)	2–4% (S)	1–4% (S)
Tau Energy Scale	–	4–15% (S)	3–8% (S)
Tau Identification	–	4–5%	1–2%
Trigger Efficiency	2–4%	2–5%	2–4%
Normalization	5%	4%–16%	9–10%
Signal			
Jet Energy Scale	1–5% (S)	3–9% (S)	2–4% (S)
Tau Energy Scale	–	2–9% (S)	4–6% (S)
Tau Identification	–	4–5%	10%
Theory	8–28%	18–23%	3–20%
Trigger Efficiency	small	small	5%

The statistical analysis of the data employs a binned likelihood function constructed as a product of the likelihood terms for each category. The likelihood in each category is a product over bins in the distributions of the  $\tau\tau$  mass. In each bin of the mass distributions, the likelihood function for the observed number of events is modeled according to a Poisson distribution based upon the expected signal and background contributions. The “signal strength” parameter ( $\mu$ ) multiplying the expected signal yield in each bin is the parameter of interest in the fit procedure. This  $\mu$  is defined as the ratio of the measured cross section normalized to the Standard Model cross section times the branching ratio for  $H \rightarrow \tau\tau$  ( $\sigma_{SM}$ ). Signal and background predictions ( $s_j$  and  $b_j$  in the  $j$ -th bin) depend on systematic uncertainties that are parametrized by nuisance parameters  $\theta$ , which in turn are constrained using Gaussian functions. The likelihood function is given by:

$$\mathcal{L}(\mu, \theta) = \prod_{\text{category}} \left[ \prod_{\text{bin } j} \text{Poisson}(N_j | \mu \cdot s_j + b_j) \prod_{\theta} \text{Gaussian}(t | \theta, 1) \right] \quad (1)$$

where  $t$  represents the auxiliary measurements, such as control regions and dedicated calibration measurements.

The expected signal and background counts dependence of the nuisance parameters is taken into account [8],

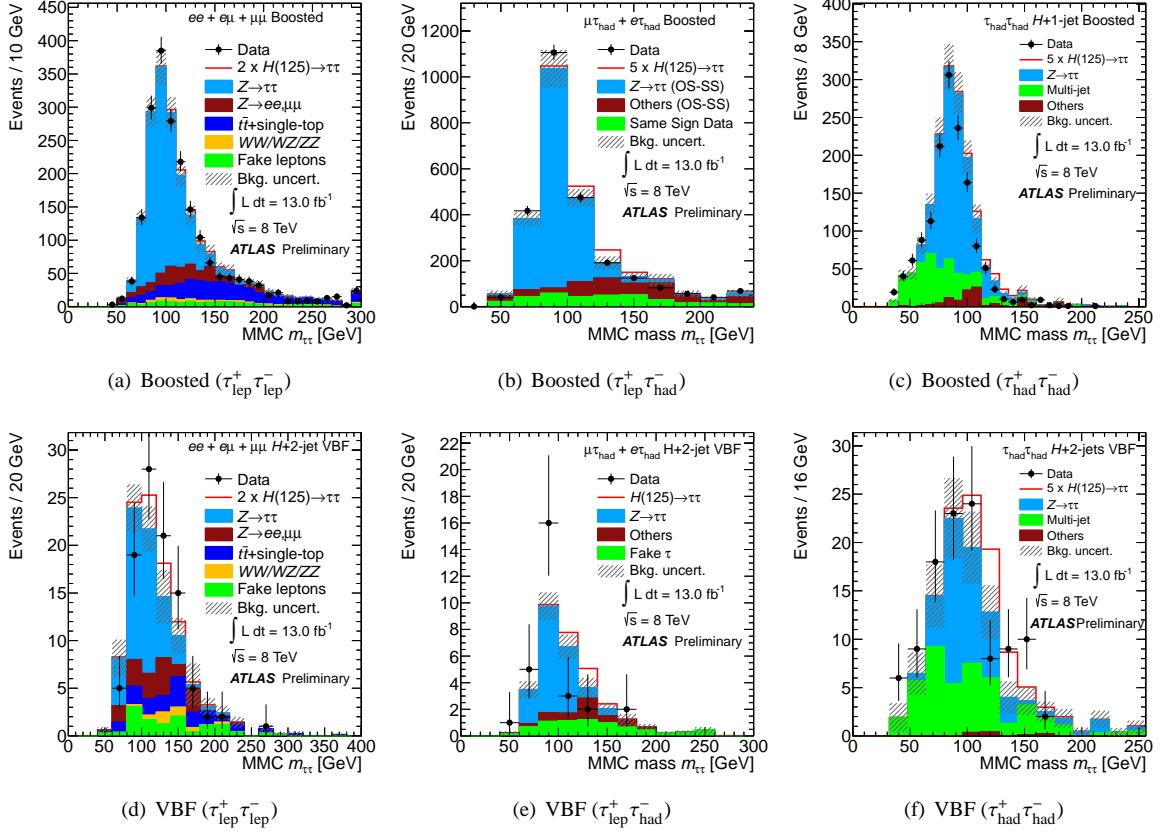


**Figure 2.** Reconstructed  $m_{\tau\tau}$  of the selected events in the 8TeV sample for the Boosted (top) and VBF (bottom) categories. Left plots show  $\tau_{\text{lep}}^+ \tau_{\text{lep}}^-$  (a,d), middle plots show  $\tau_{\text{lep}}^+ \tau_{\text{had}}^-$  (b,e) and right plots show  $\tau_{\text{had}}^+ \tau_{\text{had}}^-$ . Results are shown after all selection criteria. The signal ( $m_H = 125$  GeV) is stacked above the background contributions. The scale factors for signal, for illustration only, are given in the figure legend [4].

thus the signal and background yields are adjusted according to their best fitted values in the observed dataset.

The test statistic  $q_\mu$  is defined as:

$$q_\mu = -2 \ln \left( \frac{\mathcal{L}(\mu, \hat{\theta}_\mu)}{\mathcal{L}(\hat{\mu}, \hat{\theta})} \right), \quad (2)$$

where  $\hat{\mu}$  and  $\hat{\theta}$  refer to the global maximum of the likelihood (with the constraint  $0 \leq \hat{\mu} \leq \mu$ ) and  $\hat{\theta}_\mu$  corresponds to the conditional maximum likelihood of  $\theta$  for a given  $\mu$ . This test statistic is used to compute exclusion limits following the modified frequentist method known as  $CL_s$  [9]. The asymptotic approximation [10] is used to evaluate the Gaussian probability density functions rather than performing pseudo-experiments. This procedure has been validated using ensemble tests.

The statistical significance of an excess is evaluated in terms of the same profile likelihood test statistic. The expected sensitivity and the  $\pm 1, 2\sigma$  bands are obtained for the background expectation in the absence of a Standard Model Higgs boson signal. The consistency with the background-only hypothesis is quantified using the  $p$ -value, the probability that the test statistic of a background-only experiment fluctuates to at least the observed value.

### 3 Results

The most sensitive categories are the Boosted and VBF categories for all three channels. Distributions for the final discriminant variables are shown in figure 2 which are MMC mass distributions of the selected events. No significant excess is observed in the data compared to the SM background-only expectation in any of the channels.

Figure 3 shows the expected and observed cross section limits for a combination of all three channels as a function of the Higgs boson mass,  $m_H$ , at the 95% confidence level. The combined expected limit varies between 1.2 and 3.4 times the predicted SM cross section times branching ratio for the mass range 100-150 GeV. The corresponding observed limits are in the range between 1.9 and 3.3 times the predicted SM cross section times branching ratio for the same mass range.

The probability that a fluctuation in the background can mimic the presence of a SM Higgs boson signal is studied by calculating the local  $p_0$  value with respect to the background-only hypothesis. The values of  $p_0$  as a function of Higgs boson mass and horizontal lines showing integer value of significance in unit of  $\sigma$  are shown in figure 4. The solid and dashed lines describe the observed and expected  $p_0$  values, respectively, as a function of the Higgs boson mass corresponding to a SM Higgs boson sig-

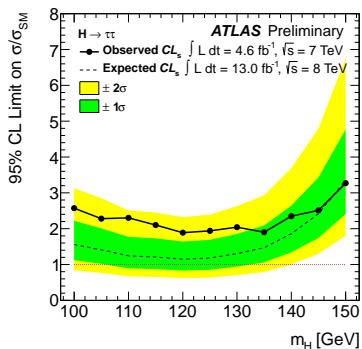


**Figure 3.** Observed (solid) and expected (dashed) 95% confidence level upper limits on the Higgs boson cross-section times branching ratio, normalized to the SM expectation, as a function of the Higgs boson mass. Expected limits are given for the scenario with no signal. The bands around the dashed line indicate the  $\pm 1\sigma$  and  $\pm 2\sigma$  uncertainties of the expected limit [4].

nal introduced with signal strength  $\mu = 1$  at the mass in question. The dotted line shows the expected  $p_0$  calculated for the case when a SM Higgs signal at  $m_H = 125$  GeV is tested as a function of the Higgs boson mass. The most significant deviation from the background-only hypothesis is observed for  $m_H = 110$  GeV with a local  $p_0$  of 7.2%, corresponding to a significance of  $1.5\sigma$ .

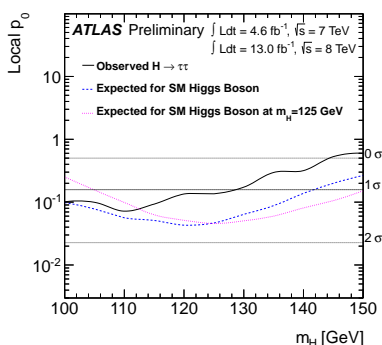


**Figure 4.** The solid and dashed lines describe observed and expected  $p_0$  values respectively, as a function of the Higgs boson mass corresponding to SM Higgs boson signal introduced with signal strength  $\mu = 1$  at the mass in question. The dotted line shows the expected  $p_0$  calculated for the case when a SM Higgs boson signal at  $m_H = 125$  GeV is tested [4].

The contributions from the different production modes in the  $H \rightarrow \tau\tau$  channel have been studied in order to assess any tension between data and the signal production cross section as predicted by the SM. Since the analysis considers three production modes,  $gg \rightarrow H$ ,  $VBF qq \rightarrow qqH$  and  $qq \rightarrow VH$ , here the latter two production modes have been grouped together as they both scale with the  $WWH$  or  $ZZH$  coupling in the SM, denoted as  $\mu_{VBF+VH}$  and the strength parameter for the remaining process is denoted as  $\mu_{ggF}$ . Two-dimensional contours in the

plane of  $\mu_{ggF} \times B/B_{SM}$  and  $\mu_{VBF+VH} \times B/B_{SM}$  are obtained as shown in figure 5, where  $B$  and  $B_{SM}$  are the measured and SM branching ratios for  $H \rightarrow \tau\tau$ . The best fit values are  $\mu_{ggF} \times B/B_{SM} = 2.4$  and  $\mu_{VBF+VH} \times B/B_{SM} = -0.4$  and the result is consistent with both SM Higgs and SM background-only hypotheses within the 95% CL contour.

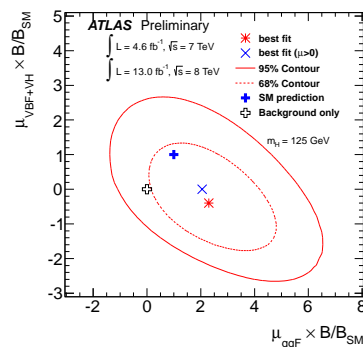


**Figure 5.** Likelihood contours for the  $H \rightarrow \tau\tau$  channel in the  $(\mu_{ggF} \times B/B_{SM}, \mu_{VBF+VH} \times B/B_{SM})$  plane are shown for the 68% and 95% CL by dashed and solid lines, respectively. The best fit to the data are shown for the case when both parameters have been constrained to non-negative ( $\times$  symbol) with contours, as well as for unconstrained case (star symbol) [4].

## 4 Conclusions

A search for a SM Higgs boson decaying in the  $H \rightarrow \tau\tau$  channels has been performed with the ATLAS detector at the Large Hadron Collider. The observed (expected) upper limit at 95% CL on the cross-section times branching ratio for SM  $H \rightarrow \tau\tau$  is found to be 1.9 (1.2) times the SM predictions for Higgs boson with mass  $m_H = 125$  GeV. For this mass, the observed (expected) deviation from the background-only hypothesis corresponds to a local significance of 1.1 (1.7) standard deviations and the best fit value of  $\mu = 0.7 \pm 0.7$ .

## References

- [1] ATLAS Collaboration, Phys. Lett. B **716** (2012) 1-29.
- [2] CMS Collaboration, Phys. Lett. B **716** (2012) 30-61.
- [3] S. Dittmaier et al., LHC Higgs Cross Section Working Group, CERN-2011-002.
- [4] ATLAS Collaboration, ATLAS-CONF-2012-160
- [5] ATLAS Collaboration, JINST **3** (2008) S08003.
- [6] R.K. Ellis, I. Hinchlie, M. Soldate and J.J. Van der Bij, Nucl. Phys. B **297** (1988) 221.
- [7] A. Elagin, P. Murat, A. Pranko, and A. Safonov, Nucl. Instrum. Meth. A **654** (2011) 481-489
- [8] K. Cranmer et al., ROOT Collaboration, CERN-OPEN-2012-16
- [9] A.L. Read, J. Phys. G **28** (2002) 2693.
- [10] G. Cowan, K. Cranmer, E. Gross, and O. Vitells, Eur. Phys. J. C **71** (2011) 1554.